Phys. Status Solidi B **250,** No. 11, 2437–2443 (2013) / **DOI** 10.1002/pssb.201349246

Part of Special Issue on
Quantum Transport at the Molecular Scale

physica status solidi b
www.pss-b.com
basic solid state physics

# Quantum transport through single atoms and molecules

**L. Vitali[1,2,3], P. Wahl[*,1,4], R. Ohmann[1,5], J. Bork[1,6,7], Y. Zhang[1,8], L. Diekhöner[6], and K. Kern[1,9]**

[1] Max-Planck-Institut für Festkörperforschung, Stuttgart, Germany
[2] Centro de Física de Materiales CFM-MPC, University of Basque Country, San Sebastián, Spain
[3] IKERBASQUE, Basque Foundation for Science, Bilbao, Spain
[4] SUPA, School of Physics and Astronomy, University of St. Andrews, North Haugh, St. Andrews, Fife, UK
[5] Insitute for Materials Science and Max Bergmann Center of Biomaterials, TU Dresden, Dresden, Germany
[6] Institut for Fysik og Nanoteknologi, Aalborg Universitet, Aalborg, Denmark
[7] Mekoprint A/S, Støvring, Denmark
[8] Department of Physics, Tsinghua University, Beijing, P. R. China
[9] Institut de Physique de la Matière Condensée, Ecole Polytechnique Fédérale de Lausanne (EPFL), Lausanne, Switzerland

Received 29 May 2013, revised 30 August 2013, accepted 2 September 2013
Published online 10 October 2013

**Keywords** nanoscale contacts, quantum transport, scanning tunneling microscopy, single atoms, single molecules

[*] Corresponding author: e-mail p.wahl@fkf.mpg.de, Phone: +49 711 689 5218, Fax: +49 711 689 1662

Experiments on quantum transport in a low temperature scanning tunneling microscope provide the possibility to study atomic and molecular contacts with well-defined electrode-geometry at least for one of the contacts, the surface. Here, we show for a number of examples, the strength of transport studies by STM. For single cobalt adatoms, we demonstrate the abrupt change in the width of the Kondo resonance of the cobalt adatom once the contact regime is reached. Differences of the mechanical properties of junctions with cobalt and gold adatoms are discussed. Finally, we show transport measurements and imaging with individual PVBA molecules.

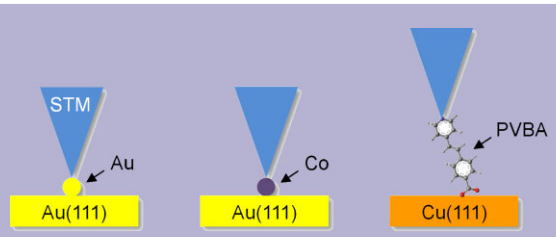


Configurations in which we have investigated quantum transport: through a junction consisting of a single gold adatom, a single cobalt adatom, and a PVBA molecule between the tip of an STM and the surface.



**1 Introduction** The integration of molecules as passive and active components in electronic circuits is one possibility to avoid a breakdown of Moores law when feature sizes approach atomic dimensions. Molecules can be designed in a versatile way to fulfill a specific functionality as a wire, molecular switch, rectifier, or even as single bit of memory. While the conceptual idea of a functional device consisting of a single molecule has been proven for single components, the practical realization of such a circuit is still facing challenging problems. While previously transport studies were mostly done in break junction experiments [1–3], in recent years a growing number of transport studies have been performed in low-temperature scanning tunneling microscopes (STM) [4–12]. Using an STM for transport studies allows selecting specific molecules through which the transport is to be investigated. Therefore, critical issues, which arise in break junctions such as how many molecules contribute to the transport, how they are anchored to the electrodes or the nature of the metal electrode can be circumvented. Theoretical studies have demonstrated that, for example, the anchoring group [13] or the conformation [14] can have substantial influence on the charge transport.

The level of control, which can be achieved by characterization of the contact area in STM offers new possibilities to optimize the transport by selecting specific "ending atoms" or adding adsorbates near the junction. These alter the electronic density of states at the sides of the molecule and induce a different response in transport. A different approach is to induce conformational changes of

the molecule trapped into the junction. A sensible increase of conductance has been observed for $C_{60}$, which had originally been attributed to deformation [9], though this interpretation is under debate [10].

An important aspect of charge transport through molecular junctions is the influence of mechanical properties of the molecule, such as stress on the molecules and details of its conformation as well as phonons. This still rather poorly investigated aspect becomes relevant if, for example, the excited vibration induces a lateral translation of the molecule [15] and possibly resulting in a loss of the contact with the electrode or when inelastic excitations promote spin flips [16]. Finally, for magnetic atoms or molecules, which carry a spin, many body effects such as the Kondo effect [8, 17–20] can have substantial influence on the transport, which is governed by the electronic states at the Fermi level. The Kondo effect leads to a strong resonance at the Fermi level, which in solids leads to an increased scattering at low temperatures and hence increased resistance, while in transport through quantum dots, it is the Kondo resonance, which enables transport in specific parameter regimes [21]. Therefore, its influence on transport differs a lot depending on the physical system under consideration.

In this paper, we present a study of quantum transport through single metal adatoms and small molecules, specifically also addressing the potential to use atomic or molecular contacts for imaging purposes and hence for a characterization of the electrode surface.

**2 Experimental** Experiments have been performed in a low temperature STM operating at 6.7 K in ultra-high vacuum with *in situ* sample transfer. Single crystal Au(111) and Cu(111) surfaces have been prepared by cycles of sputtering with $Ar^+$ ions and annealing to 800 K.

Single gold adatoms have been deposited from the tip by controlled approaching to the sample surface. This procedure has been shown previously to lead to deposition of single adatoms [7]. Cobalt adatoms have been evaporated *in situ* from a resistively heated tungsten wire, around which a cobalt wire has been wound.

4-[*trans*-2-(Pyrid-4-yl-vinyl)] benzoic acid (PVBA) molecules have been deposited *in situ* by sublimation from a crucible held at $T = 456$ K onto a Cu(111) surface at room temperature.

**3 Contacts to single gold and cobalt adatoms on Au(111)** Following preparation as described above, single adatoms of cobalt or gold are found as protrusions on the surface. Gold adatoms are imaged as ~1 Å high protrusions, cobalt adatoms are imaged with a similar height (~1.1 Å). The cobalt adatoms can be identified from tunneling spectroscopy due to their characteristic resonance near zero bias, which is interpreted as a Kondo resonance [17].

Figure 1 shows approach curves recorded with the tip positioned on top of single cobalt and gold adatoms. In both cases, we find a conductance $G_C$ in contact close to one conductance quantum $G_0 = 2e^2/h$. From the exponential

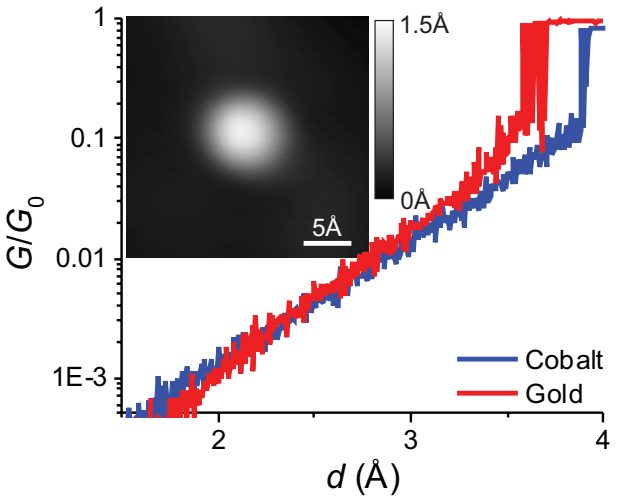


**Figure 1** Approaching curve on a cobalt and a gold adatom on Au(111). The tip is approached by a distance $d$ starting from a tunneling set point of $I = 0.1$ nA and $U = 100$ mV, at which the feedback loop is switched off. The conductance is shown on a logarithmic scale. The junction containing a cobalt atom exhibits a slightly smaller conductance compared to the one with a gold atom. Topographic STM image shows a single cobalt adatom on Au(111) ($U = 40$ mV, $I = 1$ nA).

increase of the current with the reduction of the tip–sample distance, we can extract the local barrier height between the adatoms and the tip of the STM. The behavior of the current $I$ as a function of distance $z$ is given by

$$I \propto e^{-2z\sqrt{(m/\hbar^2)2\phi}},$$

where $\phi$ the local barrier height, valid in the limit of small bias voltages. It is found that on cobalt adatoms, the local barrier height tends to be slightly smaller than on gold adatoms (compare Table 1). For both cases, an increased barrier height compared to typical values for the clean surface (~5 eV) is found, consistent with previous measurements on gold adatoms [22]. Interestingly, the conductance through a single cobalt adatom is slightly smaller than through a gold adatom.

Tunneling spectra recorded while approaching single cobalt and gold adatoms are shown in Fig. 2. The tunneling spectra acquired on single gold adatoms are featureless, and remain featureless while approaching the STM tip into contact (Fig. 2a). In contrast, spectra acquired on single

**Table 1** Local barrier height $\Phi$ measured during approach and average contact conductance $\langle G_C \rangle$ extracted from current–distance curves as shown in Fig. 1 for Au- and Co-junctions. Error bars are the standard deviation obtained by evaluating multiple curves.

| | $\Phi$ (eV) | $\langle G_C \rangle$ ($G_0$) |
|---|---|---|
| Au adatom | $7.44 \pm 2.05$ | $0.96 \pm 0.02$ |
| Co adatom | $6.16 \pm 0.56$ | $0.93 \pm 0.01$ |

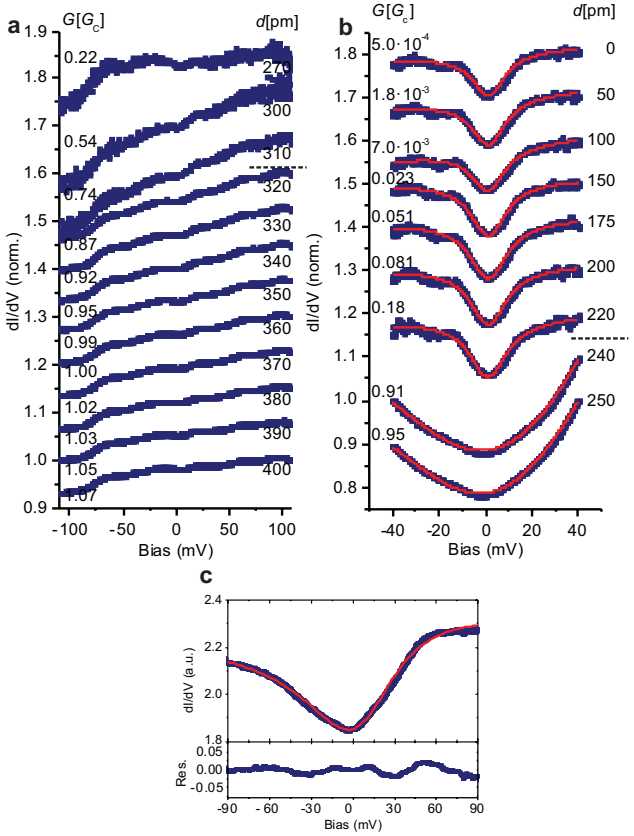


**Figure 2** Spectroscopy from tunneling to point contact for a junction containing (a) a gold adatom and (b) a cobalt adatom on Au(111) (for both the feedback loop was switched off at $U = 40$ mV, $I = 1$ nA; horizontal dashed line indicates transition from tunneling to contact, spectra in (a) and (b) are normalized and vertically offset). Next to the curves, the approaching distance after opening the feed back loop as well as the conductance in units of the conductance in contact $G_C$ is given for each curve. (c) Point contact spectrum acquired on a Co adatom in contact ($G = 1.04G_C$) at $I = 0.63$ μA, $U = 10$ mV, shown in a wider bias range than the spectra in (b). From the fit of a Fano function a width $\Gamma = 39.7 \pm 1.6$ mV has been extracted ($q = 0.27 \pm 0.02$, $\varepsilon_0 = 7.4 \pm 1.0$ mV, $a/c = 0.25 \pm 0.01$, $b$ fixed at zero, errors from the average of the parameters extracted from multiple spectra). Lower panel shows the residuum of the fit.

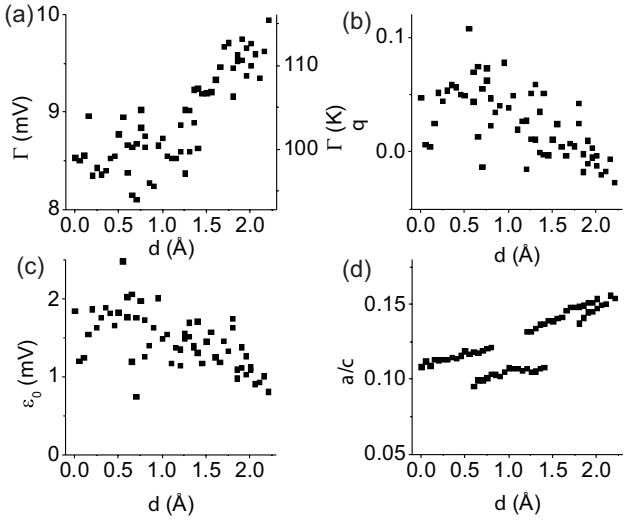


**Figure 3** Parameters of the Fano function (Eq. (1)) obtained from the fits shown in Fig. 2b (note that in Fig. 2b spectra are shown only for a selection of approaching distances for clarity). (a) Width of the resonance $\Gamma$, (b) line shape parameter $q$, (c) position of the resonance, and (d) relative amplitude $a/c$ as a function of tip approaching distance $d$. The four sections visible in Fig. 3d result from different series taken on the same atom with slight differences in the position on the atom where the spectra have been acquired (they are taken with the same tip on the same adatom).

cobalt adatoms (Fig. 2b) show a characteristic resonance [17]. The line shape of the resonance can be described by a Fano function [17, 23]

$$g(\omega) = a\frac{(\omega + q)^2}{\omega^2 + 1} + b\omega + c, \qquad (1)$$

where $\omega = (eV - \varepsilon_0)/\Gamma$, accounting in addition for a linear background. We have fitted the Fano function to the spectra for each tip–sample distance. The extracted width $\Gamma$ is shown as a function of tip approaching distance in Fig. 3a. In the tunneling regime, the width increases only slightly by ∼15% from 100 to 115 K (see Fig. 3a) when the tip is approached towards the sample. Also other parameters of the Fano line shape change only slightly (Fig. 3b–d). Upon entering the contact regime and once the conductance has jumped close to $1G_0$, the resonance broadens substantially (compare spectra taken before and after contact formation in Fig. 2b, a spectrum obtained in contact in a extended bias range is shown in Fig. 2c), the width increases by a factor of 6, whereas within the contact regime, little change in the spectra is observed. This behavior is in contrast to what has been reported for point contacts to single cobalt atoms on Cu(111) and Cu(100), where either almost no increase or only a moderate and rather smooth increase in conductance as well as in the width of the resonance has been reported [8, 18, 20]. In the data we have obtained on Au(111), similar to the jump-to-contact behavior in the current–distance transient (Fig. 1), the width increases rather abruptly once the point contact is established. A number of reasons can be responsible for the sudden increase in the width of the resonance, certainly most importantly, the coordination of the cobalt atom changes abruptly once being contacted by the second electrode, accompanied by relaxation processes in the electrodes. The changes in the Kondo temperature on different surfaces or upon contact formation have in the past been interpreted by both, changes in the hybridization [24] as well as in the position or occupation of the d-orbitals [8, 18, 25]. Since the change in the occupation of the d-orbitals appears to be rather small, as evidenced by a rather small offset of the resonance with

respect to zero bias, we expect that the dominant effect is the change in hybridization.

Point contact spectra measured with the cobalt atom in fcc and hcp positions of the surface show, within the errors, the same width of the resonance. Spectra taken on the two different positions yield widths of $39.6 \pm 0.9$ and $39.9 \pm 0.7$ mV. The only parameter, which exhibits significant differences between the two sites is the position $\varepsilon_0$ of the resonance, which is $6.8 \pm 0.9$ and $8.0 \pm 0.6$ mV.

**4 Quantum point contact microscopy with single gold and cobalt adatoms** When performing quantum point contact microscopy (QPCM) [26] with gold or cobalt adatoms, significant differences are observed. In QPCM, the tip is brought in contact with an adatom, and then scanned across the surface in constant height mode, i.e., without adjusting the tip–sample distance, while recording the current. QPCM easily achieves atomic resolution, if adatoms are used at the junction between tip and sample the images are governed by comparatively sharp contrast whenever the adatom jumps to the next hollow site. On surfaces with chemical inhomogeneity, such as surface alloys, the images reveal contrast in the transport conductance, which depends on the local chemical environment of the adatom. By QPCM, the influence of the local chemistry on quantum transport can be assessed.

For a junction consisting of a single Au atom, it is difficult to maintain a stable contact when scanning across the Au(111) surface, especially across different areas of the herringbone reconstruction. An image obtained with a Au atom as junction atom is shown in Fig. 4a. To maintain a stable contact while scanning, rather large conductances of the junction are required, at the same time, the image shows only comparatively weak contrast.

When scanning with a cobalt adatom, the junction remains significantly more stable, allowing to probe different regions of the surface reconstruction during a single scan with substantially lower contact conductances. The images exhibit more contrast than with a gold atom, showing different conductance for the fcc and hcp sites (Fig. 4b). This difference between the behavior of gold and cobalt atoms at the junction is likely due to the presence of the d-orbitals at the Fermi level in the case of a cobalt atom. These might, due to their directionality, be more sensitive to the second gold layer then is the case for a gold atom, where the valence shell has s–p character.

As pointed out in the previous section, the width of the resonance does not vary substantially between the two sites and can therefore not be responsible for the enhanced contrast, the only parameter of the Kondo resonance, which exhibits significant variation between the two sites is its position. The increased stability of the junction indicates that the bonding to the tip is stronger in case of a cobalt atom compared to a gold atom.

To disentangle what the role of site-specific relaxation of the contact atom is for the conductance in comparison with the influence of the Kondo resonance, a full-scale calculation of the tip–adatom surface junction is required.

**5 Contacts to single molecules** In the following, the quantum transport at the nanoscale will be expanded to transport through molecules. As a model system, we investigate single PVBA molecules on a Cu(111) surface. PVBA is an organic molecule consisting of a pyridyl-ring and a benzoic acid moiety bonded by a vinyl group [27–29]. The two different endgroups provide multiple reaction sites to form contacts. When deposited at room temperature the molecules deprotonate and adsorb in a planar configuration.

A topographic image is shown in the inset of Fig. 5a. The chemical groups can be clearly distinguished and the molecular structure is overlayed. To perform point-contact-spectroscopy we place the tip above selected positions of the molecule and decrease the tip–sample distance, while recording the current. Typical $I(z)$ curves are shown in Fig. 5a and b.

On first glance one can see, that they significantly differ from the case of single atoms on Cu(111). In contrast to a smooth approach curve for single adatoms, which is typically observed on Cu(111) [18], jumps in the conductance are most often observed for the molecule. Two qualitatively different $I(z)$ curves are obtained. In one case, the conductance returns to its initial value of the current after one approach–retraction cycle. In the second case, after the first jump, the curve does not revert back, but reaches a

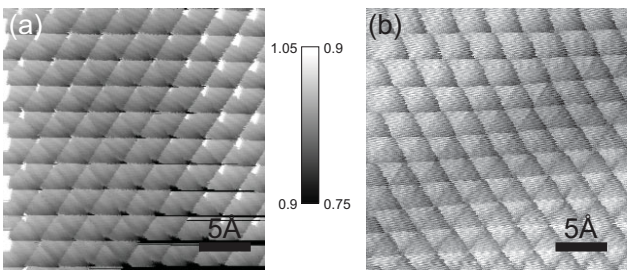


**Figure 4** Quantum point contact microscopy performed with (a) a gold atom and (b) a cobalt atom at the junction between tip and a Au(111) surface (both taken at $U = 0.1$ V; parameters prior to switching off the feedback loop: Au: $U = 0.1$ V, $I = 0.77$ μA, Co: $U = 0.01$ V, $I = 0.63$ μA). Conductances are given in units of $G_0$.

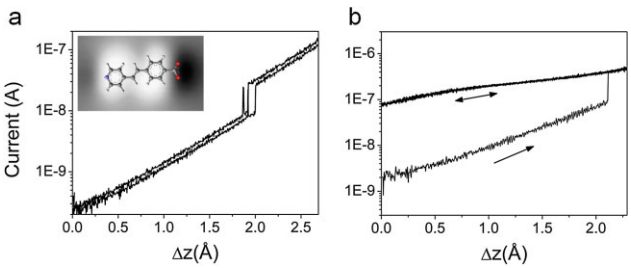


**Figure 5** Point contact spectroscopy of PVBA on Cu(111): (a) and (b) Typical current–distance curves taken on the pyridyl moiety. Bias $U = 40$ mV. Inset (a): Topographic image with the molecular structure overlayed.

higher value of the conductance. All following approach–retraction sweeps in Fig. 5b are lying on top of each other, showing that the change occurs during the first approach sweep. Variations of the transport characteristic across the single molecule were measured and are attributed to its chemical groups [30].

Here, we focus on the case when the conductance has increased after the measurement. This change is attributed to an attachment (jump-to-contact) of the molecule to the tip during the first approach [11]. The molecule is thus contacted in between tip and sample and provides additional to the tunneling current a current through the molecule. When retracting the tip further the molecule remains at the tip, which is in contrast to the case shown in Fig. 5a where the molecule reverts back to the original configuration. Subsequent topographic imaging shows the absence of the molecule from the surface, as can be seen in Fig. 6 (before (a) and after (b)). Furthermore, the image contrast has significantly changed when the molecule is attached to the tip. Atomic resolution can easily be obtained, even at moderate tunneling conditions of Bias $U = 0.35\,\mathrm{V}$ and Current $I = 0.5\,\mathrm{nA}$. Notice the dark spot at the former position of the carboxylate group. Given the strong Cu–O bond [27], a possible explanation could be the removal of one Cu atom from the surface layer.

The images taken with a molecule terminated tip depend critically on the end at which the molecule has been picked up. When the carboxylate group is attached to the tip, the pyridyl group is facing the surface and vice versa. Topographic images and respective sketches of the two configurations are shown in Fig. 7a and b. In both cases atomic resolution is obtained, however the contrast is different. In comparison to the clean tip, where no atomic resolution is obtained at these tunneling conditions, the atomic corrugation has become 10 pm (a) and can be even one order of magnitude higher up to 1 Å (b) peak to peak as can be seen in the line profiles of Fig. 7. The smooth corrugation and high resolution in (a), where the pyridyl ring faces the surface, is interpreted by tunneling through the lone pair of the N-atom [31, 32], which is strongly localized (indicated by a blue shape in the sketch). The large

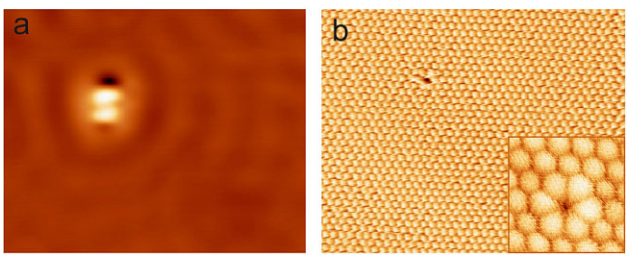


**Figure 6** Topographic images: (a) acquired with a clean metallic tip. (b) Same area, but with the molecule terminated tip. Inset: zoom in to the region of the defect. Notice the slightly larger apparent height of the atoms surrounding the defect. Tunneling conditions: (a) bias = 0.1 V, current = 0.5 nA, (b) and inset: bias = 0.35 V, current = 0.5 nA. Image sizes: $101 \times 81\,\mathrm{Å}^2$.

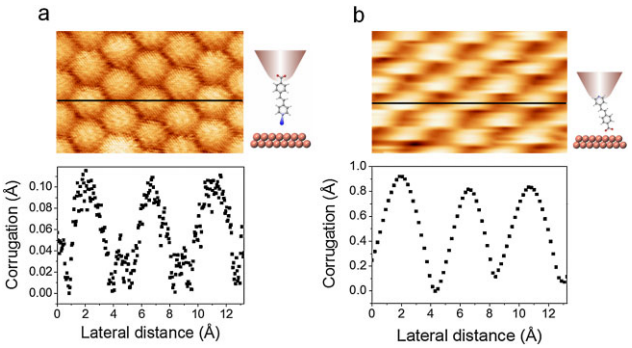


**Figure 7** (a) and (b) Topographic images of the Cu(111) surface obtained with a PVBA terminated tip in two different configurations shown together with the corresponding line cuts. The images reveal the atomic lattice of the surface. The line cuts show the atomic corrugation, which differs by an order of magnitude between the two. Imaging parameters: (a) bias = 0.35 V, current = 0.5 nA, (b) bias = 0.2 V, current = 1 nA.

corrugation with the sharp minima in (b), where the carboxylate group points to the surface, can be rationalized by a small molecule–surface distance. While the tip moves along the surface with the molecule at the apex of the tip, the free end of the molecule slides along the surface. The sharp features and the large corrugation indicate that the end of the molecule which is on the surface prefers to remain in specific sites, from where it hops to an adjacent site once the tip has moved sufficiently far. Once the molecule is in a preferred site, the profile is smooth during the time the tip moves until the molecule jumps to the next site, visible as a sharp minimum. This process is then repeated leading to the atomic resolution. Thus while the imaging mode differs from QPCM, the contrast mechanism is similar. From the observed pattern, the preferred adsorption site is likely on top of the copper atoms.

The measurements were performed on a single crystal surface, where all atoms are equal. Given the possibility to identify defects, one can expect to see contrast between different kinds of atoms.

Comparing the extension of the piezo scanner for the clean and molecule terminated tip, one finds that the tip has to be moved further away from the sample with the molecule attached to the tip to achieve the same tunneling current. For several pick up events on different molecules with microscopically different tips the additional separation from the sample is $6 \pm 1$ Å. This value is much lower than the length of the molecule (11.5 Å) [29]. There are two possible reasons: first, the molecule is not directly attached to the apex of the tip, but sideways or in a tilted configuration. Secondly, besides geometrical considerations electronic effects play a role. The charge transport through the molecule is different from a tip simply extended by several additional metal atoms. Additionally, the overlap of wave functions of the molecule acting as a tip apex is different than with a metal tip, which has only metallic states [33]. Along a molecule

composed of aromatic rings, with alternating single and double carbon bonds, the transport is described via an off-resonant tunneling mechanism. The conductance scales inversely proportional to the exponential of the length of the molecule [34]. While the functional behavior is similar to a vacuum tunneling junction, it occurs with a different exponential prefactor. Using the damping prefactor as shown in Ref. [35] would result in a reduction of the conductance by two orders of magnitude while retracting the tip by the full length of the PVBA molecule (on the order of 1 nm). The apparent length is then reduced by approximately two Angstrom with respect to the original length of the molecule. This is in qualitative agreement with the observed lower values of the length.

To measure the transport through the molecule attached to two electrodes (here, tip and surface) the tip, holding the molecule, is brought closer to the surface. Conductance curves such as shown in Fig. 8 are then obtained. In an initial region of several Angstrom the conductance shows small variations (jumps), but stays more or less constant (within one order of magnitude). This is in contrast to the exponential behavior expected from tunneling through vacuum (see dashed line). When approaching closer, another regime is reached, marked by the dotted line, where the conductance follows an exponential. The first regime indicates an additional current flow, which amounts to $10^{-4}\,G_0$. This can be considered as the conductance through the molecule. The small jumps are indicative of a sliding motion of the molecule across the surface, which binds to new atomic sites. Once the tip is brought sufficiently close the tunneling between tip and sample will dominate. The potential barrier in this case is lowered with respect to the "clean" tip, due to the presence of the molecule at the tip.

The STM experiments with PVBA on Cu(111) show a variety of conductance–distance curves, indicating the complexity that is encountered when molecular adsorbates are contacted with the STM electrode. Nevertheless, the measurements were reproducible and several key behaviors could be identified.

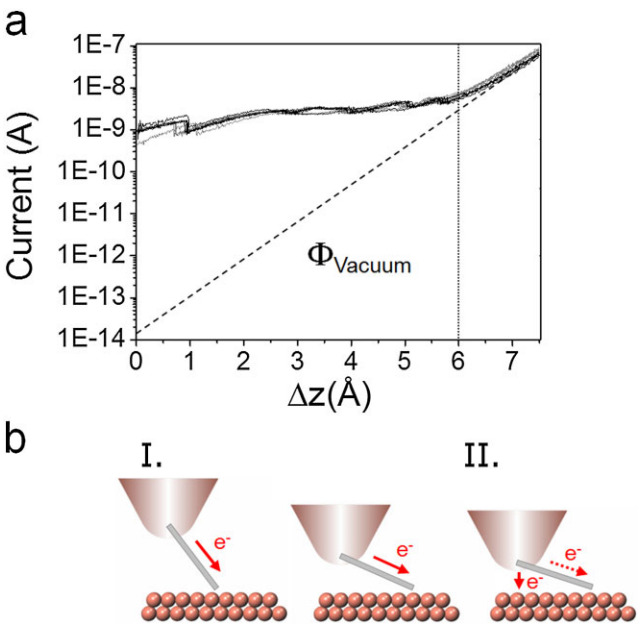


**Figure 8** (a) Quantum transport through the molecule. Approach (retraction) sweeps of the molecule terminated tip toward (black lines) (away from (gray lines)) the surface. The presented sweeps were performed directly after each other on the same molecule. After an initial sliding of the molecule across the surface, where the transport through the molecule dominates, a second regime is reached (dotted line), when the tunneling from the tip to the sample becomes large enough. Bias = 100 mV. (b) Model of the process when retracting the tip. The picture labeled II corresponds to the regime where both, transport through the molecule as well as vacuum tunneling contribute, whereas the two panels labeled I are in the regime dominated by transport along the molecule.

**6 Conclusions** We have shown contact formation and transport properties of reversible contacts to single cobalt and gold atoms as well as of PVBA molecules and discussed imaging in transport through both, single atoms and molecules. While the gold atoms are non-magnetic, and transport spectroscopy shows essentially the same structure as tunneling spectroscopy, for cobalt atoms significant changes in the Kondo effect are observed – stronger than in most other previously studied contacts to cobalt adatoms. Transport studies of organic molecules, exemplarily PVBA molecules, reveal a distinctly different behavior. PVBA molecules exhibit conductances, which are at least an order of magnitude smaller than for adatoms. We demonstrate imaging with a single PVBA molecule on the tip, achieving atomic resolution with substantially smaller conductances compared to atoms.

**Acknowledgements** We acknowledge support by the Deutsche Forschungsgemeinschaft (DFG) through SPP1243. Y.H.Z. acknowledges support by the Chinese Scholarship Council.

## References

[1] M. A. Reed, C. Zhou, C. J. Muller, T. P. Burgin, and J. M. Tour, Science **278**, 252 (1997).
[2] J. Reichert, R. Ochs, D. Beckmann, H. B. Weber, M. Mayor, and H. v. Löhneysen, Phys. Rev. Lett. **88**, 176804 (2002).
[3] R. H. M. Smit, Y. Noat, C. Untiedt, N. D. Lang, M. C. van Hemert, and J. M. van Ruitenbeek, Nature **419**, 906 (2002).
[4] J. K. Gimzewski and R. Möller, Phys. Rev. B **36**, R1284 (1987).
[5] A. Yazdani, D. M. Eigler, and N. D. Lang, Science **272**, 1921 (1996).
[6] L. Bürgi, PhD Thesis, EPFL Lausanne (1999).
[7] L. Limot, J. Kröger, R. Berndt, A. Garcia-Lekue, and W. A. Hofer, Phys. Rev. Lett. **94**, 126102 (2005).
[8] N. Néel, J. Kröger, L. Limot, K. Palotas, W. A. Hofer, and R. Berndt, Phys. Rev. Lett. **98**, 016801 (2007).
[9] C. Joachim, J. K. Gimzewski, R. R. Schlittler, and C. Clavy, Phys. Rev. Lett. **74**, 2102 (1995).
[10] N. Néel, J. Kröger, L. Limot, T. Frederiksen, M. Brandbyge, and R. Berndt, Phys. Rev. Lett. **98**, 065502 (2007).

 

[11] F. Pump, R. Temirov, O. Neucheva, S. Soubatch, S. Tautz, M. Rohlfing, and G. Cuniberti, Appl. Phys. A **93**, 335 (2008).
[12] L. Vitali, R. Ohmann, K. Kern, A. Garcia-Lekue, T. Frederikson, D. Sanchez-Portal, and A. Arnau, Nano Lett. **10**, 657 (2010).
[13] G. Kim, S. Wang, W. Lu, M. B. Nardelli, and J. Bernholc, J. Chem. Phys. **128**, 024708 (2008).
[14] J. J. Palacios, A. J. Pérez-Jiménez, E. Louis, and J. A. Vergés, Nanotechnology **12**, 160 (2001).
[15] T. Komeda, Y. Kim, M. Kawai, B. N. J. Persson, and H. Ueba, Science **295**, 2055 (2002).
[16] A. J. Heinrich, J. A. Gupta, C. P. Lutz, and D. M. Eigler, Science **306**, 466 (2004).
[17] V. Madhavan, W. Chen, T. Jamneala, M. F. Crommie, and N. S. Wingreen, Science **280**, 567 (1998).
[18] L. Vitali, R. Ohmann, S. Stepanow, P. Gambardella, K. Tao, R. Huang, V. S. Stepanyuk, P. Bruno, and K. Kern, Phys. Rev. Lett. **101**, 216802 (2008).
[19] J. Bork, Y. Zhang, L. Diekhöner, L. Borda, P. Simon, J. Kroha, P. Wahl, and K. Kern, Nature Phys. **7**, 901 (2011).
[20] D.-J. Choi, M. V. Rastei, P. Simon, and L. Limot, Phys. Rev. Lett. **108**, 266803 (2012).
[21] D. Goldhaber-Gordon, H. Shtrikman, D. Mahalu, D. Abusch-Magder, U. Meirav, and M. A. Kastner, Nature **391**, 156 (1998); S. M. Cronenwett, T. H. Oosterkamp, and L. P. Kouwenhoven, Science **281**, 540 (1998).
[22] J. Kröger, H. Jensen, and R. Berndt, New J. Phys. **9**, 153 (2007).
[23] O. Újsághy, J. Kroha, L. Szungyogh, and A. Zawadowski, Phys. Rev. Lett. **85**, 2557 (2000).
[24] P. Wahl, L. Diekhöner, M. A. Schneider, L. Vitali, G. Wittich, and K. Kern, Phys. Rev. Lett. **93**, 176603 (2004).
[25] N. Knorr, M. A. Schneider, L. Diekhöner, P. Wahl, and K. Kern, Phys. Rev. Lett. **88**, 096804 (2002).
[26] Y. Zhang, P. Wahl, and K. Kern, Nano Lett. **11**, 3838 (2011).
[27] L. Vitali, G. Levita, R. Ohmann, A. Comisso, A. De Vita, and K. Kern, Nature Mater. **9**, 320 (2010).
[28] R. Ohmann, L. Vitali, and K. Kern, Nano Lett. **10**, 2995 (2010).
[29] R. Ohmann, G. Levita, L. Vitali, A. De Vita, and K. Kern, ACS Nano **5**, 1360 (2011).
[30] L. Vitali, R. Ohmann, M. Tododrovic, R. Perez, and K. Kern, in preparation.
[31] B. J. Bandy, D. R. Lloyd, and N. V. Richardson, Surf. Sci. **89**, 344 (1979).
[32] L. J. Lauhon and W. Ho, J. Phys. Chem. A **104**, 2463 (2000).
[33] L. Gross, N. Moll, F. Mohn, A. Curioni, G. Meyer, F. Hanke, and M. Persson, Phys. Rev. Lett. **107**, 086101 (2011).
[34] M. Magoga and C. Joachim, Phys. Rev. B **56**, 4722 (1997).
[35] L. Lafferentz, F. Ample, H. Yu, S. Hecht, C. Joachim, and L. Grill, Science **323**, 1193 (2009).